Deliverable D 3.1
Discrete element model of a typical refractory microstructure

Document type	**Deliverable D 3.1**
Document Version / Status	**2.3**
Primary Authors	**Marc Huger,** marc.huger@unilim.fr, **UNILIM**
Distribution Level	**PU (Public)**
Project Acronym	**ATHOR**
Project Title	**Advanced THermomechanical multiscale mOdelling of Refractory linings**
Grant Agreement Number	**764987**
Project Website	www.etn-athor.eu
Project Coordinator	**Marc Huger,** marc.huger@unilim.fr, **UNILIM**
Document Contributors	**Marc Huger,** marc.huger@unilim.fr, **UNILIM** **Farid Asadi,** farid.asadi@unilim.fr, **UNILIM**

History of Changes

Version	Date	Author (Organization)	Change	Page
1.0	27/01/2021	Farid ASADI, (UNILIM, IRCER)	Defining the outlines	All
1.1	15/02/2021	Farid ASADI, (UNILIM, IRCER) Marc HUGER, (UNILIM, IRCER)	Checking outlines and context	All
2.0	28/02/2021	Farid ASADI, (UNILIM, IRCER)	Adding the detailed contents	All
2.1	01/03/2021	Farid ASADI, (UNILIM, IRCER) Marc HUGER, (UNILIM, IRCER)	Revising the document	All
2.2	04/03/2021	Farid ASADI, (UNILIM, IRCER) Marc HUGER, (UNILIM, IRCER)	Revising the document	All
2.3	26/03/2021	Glyn DERRICK, (UNILIM, IRCER)	Final English check	All

European Commission | Horizon 2020 European Union funding for Research & Innovation

TABLE OF CONTENTS

1 Introduction

As an output of WP3, dedicated to “Innovative modelling from microstructure to industrial scale”, this report will review the development of the numerical tool (Task 3.1) based on the Discrete Element Method (DEM) to investigate the role played by the microstructure (i.e. grain size, grain properties and interface characteristics) in the macroscopic thermomechanical behaviour. This approach will be compared with laboratory prepared, model materials submitted to various mechanical testing coupled with experimental observations, in particular digital image correlations. This model could be used, in a loop, to define the optimal microstructure to enhance the macroscopic characteristics identified as critical from the point of view of the vessel lifespan.

2 Numerical framework and the chosen contact model

In the early stages of this project, GranOO[1] (a free DEM workbench) was used as the simulation tool. This was due to the fact that, in IRCER (Institut de Recherche sur les Céramiques, Limoges, France), the thermomechanical research group already had some experience in developing GranOO. However, by reviewing other potential DEM contact models, the recently developed Flat Joint Model (FJM) [1] showed greater potential for the goals of this deliverable. Initially, the FJM was introduced to mimic the microstructure of angular, interlocked grains, similar to marble, in the context of geomechanics. This concept of mimicking such interlocked granular materials was, in fact, very close to the general microstructure of refractories (large interlocked aggregates within a finer matrix). This FJM is implemented within a software called Particle Flow Code (PFC)[2] from ITASCA company. In this section, firstly, the Flat Joint Model (FJM) and its input parameters will be introduced. Afterwards, a rationalised trial and error calibration process for FJM local parameters will be proposed.

2.1 Flat Joint contact Model (FJM)

FJM can simulate the microstructure of interlocked grains within a material thanks to the flat contact interfaces. This feature allows the model to exhibit translational and rotational frictions between discrete elements. This key point made this contact model suitable for the present study, targeting multiscale simulation of partially damaged grain-based materials, like refractories. The detailed formulation of FJM has been explained in the PFC code documentation [2]; therefore, the main points of this model will be presented here.

[1] https://www.granoo.org/

[2] https://www.itascacg.com/software/PFC

European Commission | Horizon 2020 European Union funding for Research & Innovation

Commonly, a flat-jointed bonded numerical material is built up from a compacted granular assembly of spherical discrete elements. Before assigning FJM between nearby discrete elements within this assembly, an initial small distance gap (g_0) is set up to define which discrete elements should be bonded. Thus, an FJM bonded contact is created if the distance between two discrete elements is smaller than this assigned initial gap (g_0), as shown in Fig. 1 (b). This g_0 value has a significant influence on the connectivity of the discrete elements of the assembly and thus, could significantly influence the relation between local and apparent property. As an illustration, if g_0 is initially set to zero, only the touching (or slightly overlapping) elements will be bonded. Therefore, it is preferable to assign a non-zero value as a bonding gap, usually set to a given ratio of the average of discrete elements size.

An FJM contact is built up from a certain number of contacting sub-surfaces (referred to as "*elements*" in PFC technical documentation, which use thus superscript "*e*" in later formulations) which could carry forces and moments that obey the force-displacement law. For example, in Fig. 1 (a), the FJM contact could be considered partially damaged as some sub-surfaces are "unglued". In the unglued configuration, the concerned sub-surface is not able to transmit attractive tensile forces, while it can still transmit repulsive compressive forces. As a result of this planar contact geometry associated with sub-surfaces, it is possible to model resistance against rotations to mimic a grain-based interlocked assembly.

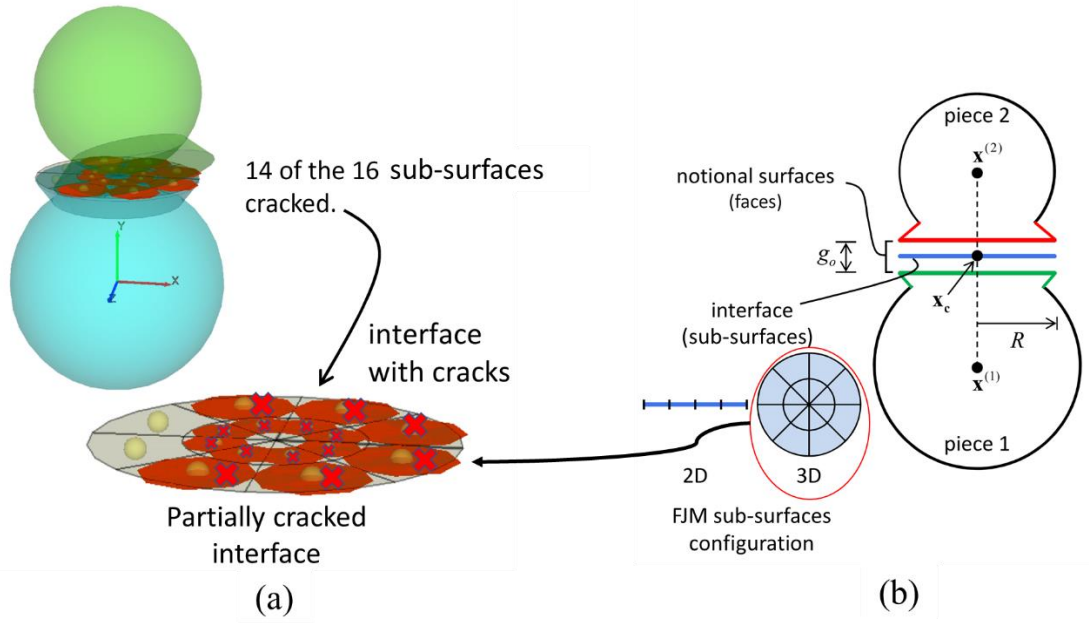

Fig. 1. The FJM contact: (a) focus on a partially damaged flat joint, and (b) the schematic basis of the FJM, adapted from [2].

As shown in Fig. 1 (a), a full FJM bonded contact in 3D is built up from 16 sub-surfaces. The fracturing criterion of a single sub-surface in FJM is shown in Fig. 2. This criterion is inspired from the classical truncated Mohr-Coulomb theory, which is represented in the shear stress ($\tau^{(e)}$) vs compression stress ($-\sigma^{(e)}$) plane and adapted to rock mechanics, for which compression is considered positive (tension being thus negative). The parameters t^{loc}, c^{loc} and ϕ^{loc} correspond to the tensile strength, the cohesion and the friction angle used locally as rupture criteria for each single sub-surface.

Before rupture, each single sub-surface exhibits a linear elastic mechanical behaviour (based on K_n^{loc} corresponding to the normal stiffness and K_s^{loc} to the shear stiffness) until its equivalent stress in the Mohr-Coulomb stress space reaches the limit. Then, the sub-surface is considered unglued and detached. A detached FJM sub-surface can no longer carry tensile stresses. However, the detached sub-surface still can be active in compression with associated friction.

European Commission | Horizon 2020 European Union funding for Research & Innovation

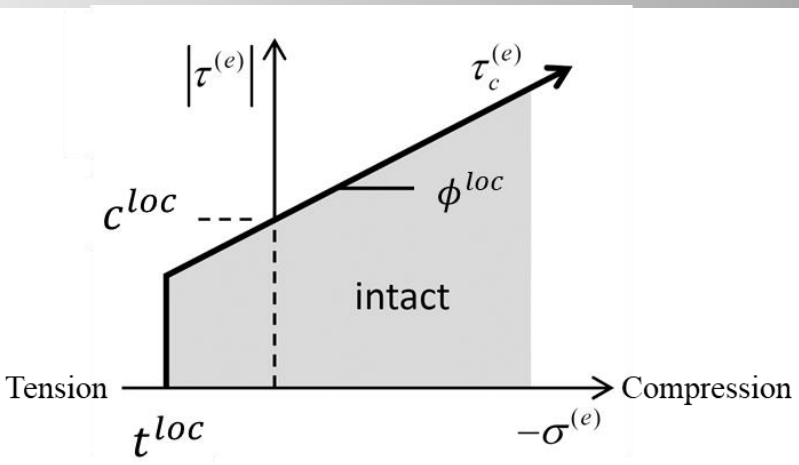

Fig. 2. Typical Mohr-Coulomb graph and associated different fracturing criteria used for a single FJM sub-surface

The global rheological model of each FJM sub-surface is summarised in Fig. 3. For a given FJM bond, all of its 16 sub-surfaces follow the same rheological model and share the same parameter values of K_n^{loc}, K_s^{loc}, t^{loc}, c^{loc} and ϕ^{loc}. These local input parameters are marked by superscript "*loc*", in contrast with apparent macroscopic properties, marked by superscript "*ap*".

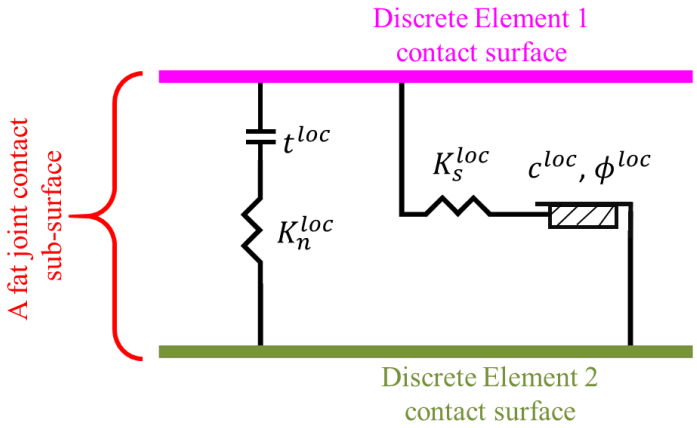

Fig. 3. Bonded flat joint contact: the rheological model and the associated parameters, adapted from [2]

The list of FJM bonded contact parameters that were used in this study are shown in Table 1.

Table 1. The input parameters in the Flat Joint contact model

Parameter description	Symbol	Elastic / fracture	Unit
Initial gap	g_i^{loc}	-	m
Normal stiffness of bond	K_n^{loc}	Elastic	N/m
Shear stiffness of bond	K_s^{loc}	Elastic	N/m
Local Young's modulus of bond	E^{*loc}	*Elastic*	*GPa*
Local stiffness ratio (K_n^{loc}/K_s^{loc}) of bond	K^{*loc}	*Elastic*	-
Local tensile strength of bond	t^{loc}	Fracture	MPa
Local cohesion of bond	c^{loc}	Fracture	MPa
Local friction angle	ϕ^{loc}	Fracture	Degrees

2.2 Rationalised trial and error calibration process for FJM

Generally, the main disadvantage of DEM approaches is the lack of well-defined relationships between the contact properties (the local parameters of the bonds between discrete elements) and the apparent brittle elastic properties, which are related to the simulated material. In this way, the FJM requires a calibration process to assign the correct values for the contact properties to reproduce the desired apparent brittle elastic properties. Due to the high number of local input parameters of the FJM and of the

European Commission | Horizon 2020 European Union funding for Research & Innovation

complex interdependencies of these parameters on the apparent behaviour, no direct calibration process has been proposed for FJM yet. Nevertheless, an indirect calibration algorithm has been recently proposed by V. Andres *et al.* [3]. From this work, an improved indirect calibration algorithm is proposed here in order to adjust the local input parameters to apparent targeted properties. The proposed algorithm (shown in Fig. 4) considers the different calibration steps for the most influential local parameters involved in the targeted goals of this study.

The very preliminary step for the calibration is to fix the numerical sample geometry. Then, the modelled sample should be mechanically loaded in order to obtain the apparent mechanical behaviour targeted for the material. It should be mentioned that the calibration process proposed in Fig. 4 is exclusively focused here on tensile behaviour. In fact, this deliverable is dedicated to refractory materials, which are well-known to be more sensitive in tension (mode I). Thus, the local input parameters which influence the apparent compressive strength (c^{loc} and ϕ^{loc}) have been intentionally excluded from the proposed calibration process.

The proposed calibration of FJM contact model parameters follows a systematic step by step approach where each step is detailed below.

1. *Initial gap* (g_i^{loc}): assigning a small value for the bonding gap will result in an asymmetric rigidity between compression and tension, which is unwanted for the purpose of this study.
2. *Local stiffness ratio* (K^{*loc}): in the second step, the local stiffness ratio (K^{*loc}) is calibrated. This parameter greatly influences the apparent Poisson's ratio (ν^{ap}) [4].
3. *Local Young's modulus* (E^{*loc}): after calibrating and fixing the local stiffness ratio (K^{*loc}), the local Young's modulus (E^{*loc}) should be set to a value that produces the targeted apparent Young's modulus (E^{ap}).
4. *Local tensile strength* (t^{loc}): finally, after calibrating the elastic properties, the targeted apparent tensile strength (t^{ap}) is calibrated by changing the local tensile strength (t^{loc}).

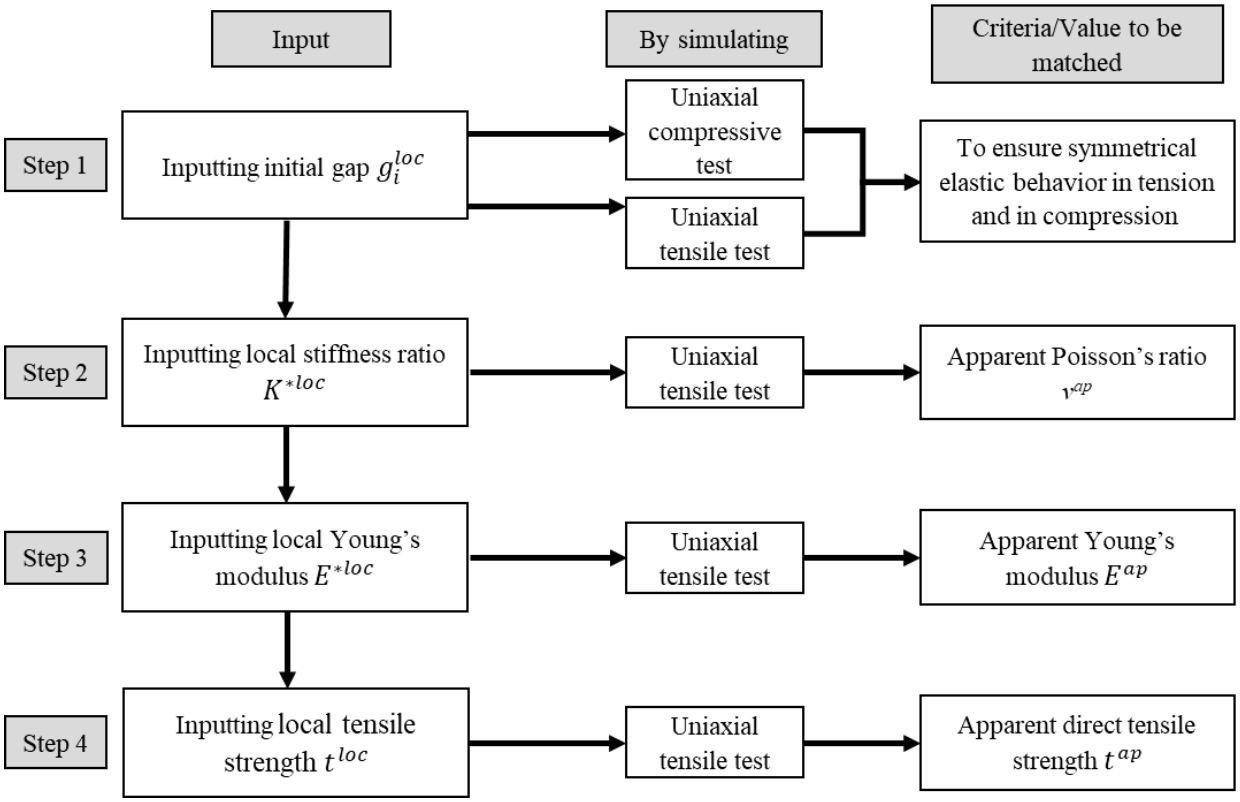

Fig. 4. The modified algorithm to calibrate apparent brittle elastic parameters of the numerical sample inspired from [3].

3 Modelling the elastic properties of bi-phase (and porous) refractories by using periodic homogenisation approach in DEM

The heterogeneous microstructure of refractories significantly influences their ability to sustain thermal shocks in their application. The thermal expansion mismatch between constituents (large aggregates within a matrix), leading to microcracking around the

European Commission | Horizon 2020 European Union funding for Research & Innovation

aggregates, allows for improved thermal shock resistance. Therefore, to define the most suitable microstructure design, a rational experimental procedure of optimisation, working with model materials containing only a limited number of constituents called "model materials" (see section 3.1), has been considered. In fact, despite the simplified microstructure of the model materials, they could exhibit a thermomechanical behaviour that can mimic some aspects of industrial refractories behaviour. Hence, it is crucial to understand better the strong relationships between such microstructures and the macroscopic thermomechanical behaviour of these model materials. Beyond this experimental procedure of optimisation, evidently, the DEM numerical modelling can help to have a better view of such complex phenomena.

The homogenisation aspect in DEM is still today not as robust as in FEM. In this way, one of the first goals of WP3 was to carefully investigate the elastic properties (Young's modulus, Poisson's ratio, and potential anisotropy) from the micro-scale (related to local inclusions or pores) to the macro-scale (related to the volume fraction of inclusions or pores). Hence, to achieve such local to apparent (micro to macro) multiscale simulations in DEM, a dedicated numerical approach was proposed.

The implementation of the periodic homogenisation approach in DEM allows working on a pseudo-infinite domain with a limited number of discrete elements by replicating a representative volume cell (see section 3.2.2). Thus, this approach enables such cross-scale transition from the unit cell to the infinite domain. Here, the elastic properties of bi-phase (and porous) materials will be investigated as a first study in order to validate such an original approach with DEM (not so well-documented at the moment). In fact, validating such an approach will be an opening to introduce later the thermal damages resulting from thermal expansion mismatch between constituents in order to study the effect on thermal shock resistance. As mentioned, in such a perspective, the Flat Joint DEM contact model was chosen as it is capable of reproducing realistic crack initiation and propagation at a micro-scale.

To compare the accuracy and the efficiency of this proposed homogenisation approach in DEM, the given apparent elastic properties will be compared to experimental results measured on real model materials: bi-phase material (see section 3.1). Finally, the obtained numerical results will be compared to an analytical model and to FEM simulations.

3.1 Bi-phase model material for consolidating the homogenisation approach

The microstructures of refractory materials are having complex couplings between aggregates and matrix, which affect different macroscopic properties of the material. Thus, to study the elastic properties of bi-phase materials, it was necessary to design and produce a simplified material called "model material". In such simplified materials, only the thermomechanical interactions of two solid phases are expected. This simplification was required in order to clearly observe the effect of increasing the inclusions fraction (or porosity) on the elastic macroscopic response of the materials.

To study elastic behaviour of the bi-phase material regarding the inclusions fraction and porosity, Tessier-Doyen et al. [5] have designed and built a bi-phase "model material". This bi-phase material with solid inclusions was a Glass matrix with Alumina inclusions (G/A). This model material is made from the composition of a dense aluminosilicate glass matrix containing randomly distributed single-sized spherical alumina beads (with a mean diameter of 500 µm). The elastic properties of each phase are shown in Table 2. Different samples of this material have been produced by varying inclusion fractions in order to observe the effect on the apparent elastic behaviour of the material. The microstructure of this model material has been shown in Fig. 5 (a) for 28 % of the inclusion volume fraction.

European Commission | Horizon 2020 European Union funding for Research & Innovation

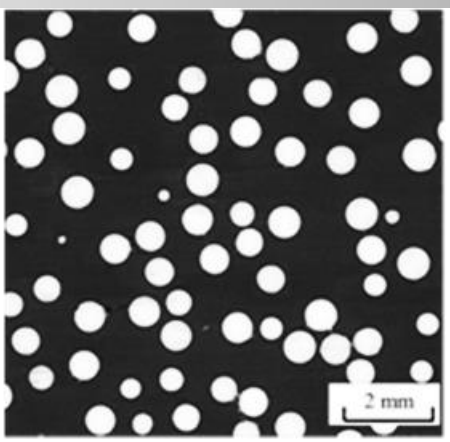

Fig. 5. Model bi-phase materials: glass matrix with spherical alumina inclusions [6].

Table 2. Measured properties of constituents of model bi-phase materials [6].

Property		Measured model material property
Matrix (Glass)	Young's modulus	78 GPa
	Poisson's ratio	0.206
Inclusions (Alumina)	Young's modulus	340 GPa
	Poisson's ratio	0.240

3.2 Numerical methods for homogenisation applied to DEM

In this section, some of the numerical methods and techniques which are required to apply the homogenisation to DEM models are explained. At first, the periodic boundary conditions (PBC) will be explained (section 3.2.1), then a Representative Volume Elements (RVE) will be chosen and built to be used with the Periodic Boundary Conditions (PBC) (section 3.2.2).

3.2.1 Periodic Boundary Condition (PBC) in the Discrete Element Method (DEM)

In numerical models, periodic boundaries are often used to remove free boundary effects [7]. Theoretically, in a PBC applied to a DEM model, if a discrete element centroid goes outside the periodic boundary box, it translates back to the opposite face of the box. In order to ensure contacts between element located at opposite faces (or corners) of the boundary, "ghost" elements are introduced [2]. The ghost elements are shown in red in Fig. 6 for a perfect 2D square RVE. The blue square at the centre of the picture is called a unit cell.

European Commission | Horizon 2020 European Union funding for Research & Innovation

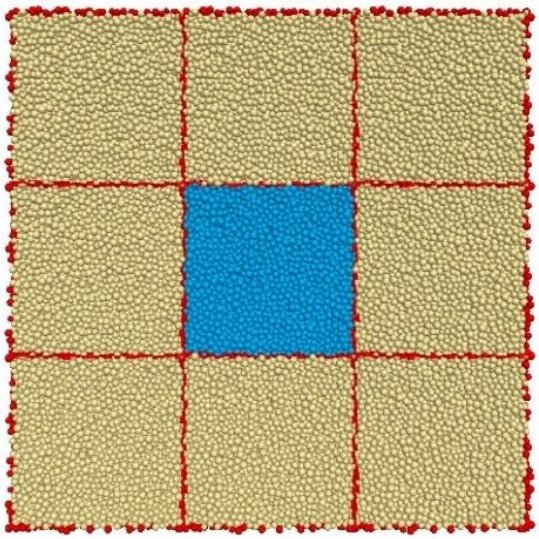

Fig. 6. A square specimen in PBC (in 2D). Ghost elements and PBC borders are shown in red. The main RVE is in blue (only 8 copies are shown here in 2D; However, 26 copies should be considered in 3D).

3.2.2 *Creating Representative Volume Elements (RVE)*

For building the unit cell in the periodic 3D space for homogenisation technique, it was necessary to choose a periodic microstructure arrangement that induces a low degree of anisotropy in order to reproduce a statistically isotropic behaviour of the bi-phase material (see section 3.1). Based on the previous studies, a Face-Centred Cubic (FCC) arrangement had shown a low degree of anisotropy for periodic homogenisation [8]. Therefore, the FCC arrangement has been chosen for the present study to represent a bi-phase material (matrix-inclusion system) RVE. In Fig. 7, the matrix is shown in blue, and the inclusions are in grey.

To create a bi-phase RVE with two different constituents, it was necessary to assign different contact (local) properties for the matrix and inclusion regions. Local values were obtained independently by going through the calibration process in PBC for each constituent separately. The interface properties (the contacts between inclusion elements and matrix elements) could be assigned as the matrix, the inclusions, or other desired properties. In this study, for these interface contacts, the matrix properties have been assigned. In other words, no particular property was given to the interface. In fact, in the present case, for which no particular properties have been targeted for the interface during the processing of the model material and thus promoting a very good/strong bond of the glass matrix (by sintering) on the surface of the Alumina beads, properties of the interface could be assumed similar to the matrix. The contact network is shown in Fig. 7 (c), where the interface contacts are shown explicitly in red.

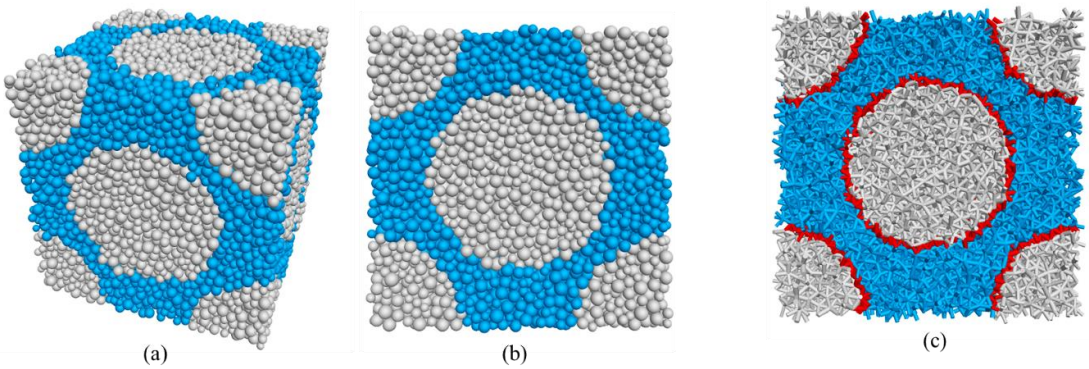

Fig. 7. FCC arrangement: (a) and (b) numerical sample produced by around 20k discrete elements, and (c) the contacts among the discrete elements.

It is noteworthy to mention that the total number of 20k discrete elements was enough for this RVE, considering the computation time efficiency and accuracy of results. The proposed study aims to compare the influence of the inclusion volume fraction on the apparent elastic properties of the model with an analytical model and experimental observations. In such a perspective, several inclusion radii were considered inside the RVEs (Fig. 8).

European Commission | Horizon 2020 European Union funding for Research & Innovation

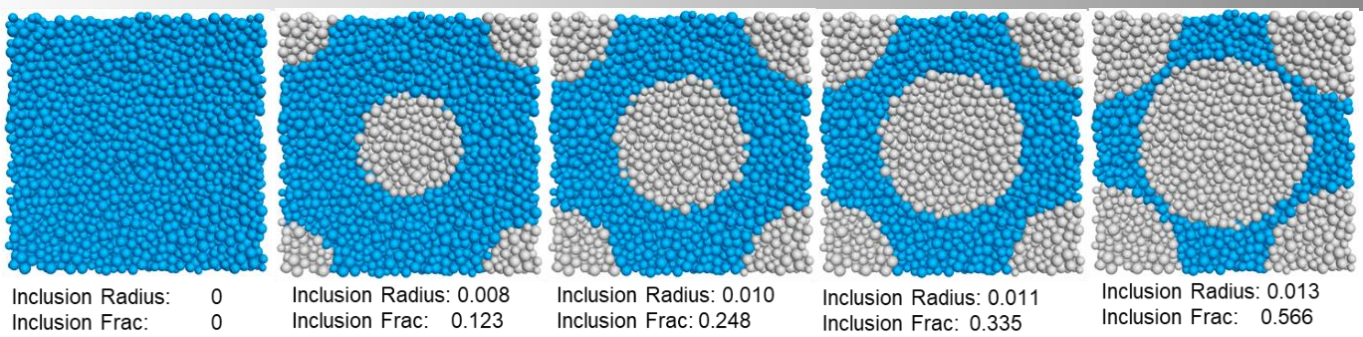

Fig. 8. Illustrations of some numerical samples with different inclusion fractions, increasing from 0 % to 57 % in an FCC arrangement.

3.3 Elastic properties obtained by DEM using PBC confronted with reference values

In this section, the results of the simulation of the model material with stiffer inclusions (glass matrix with alumina spherical inclusions G/A) have been investigated. Theoretically, by increasing the inclusion fraction in the RVEs, the results should follow the lower Hashin and Shtrikman bound (HS-) [9] [10] [11], which is considered as an analytical reference for bi-phase materials. Therefore, the inclusion fraction has been increased within the DEM model RVEs as well as the FEM model. Afterwards, results obtained from these simulations have been compared to the experimental reference values. It should be noted that both DEM and FEM models were based on FCC-arranged RVEs. All results are shown in Fig. 9.

European Commission | Horizon 2020 European Union funding for Research & Innovation

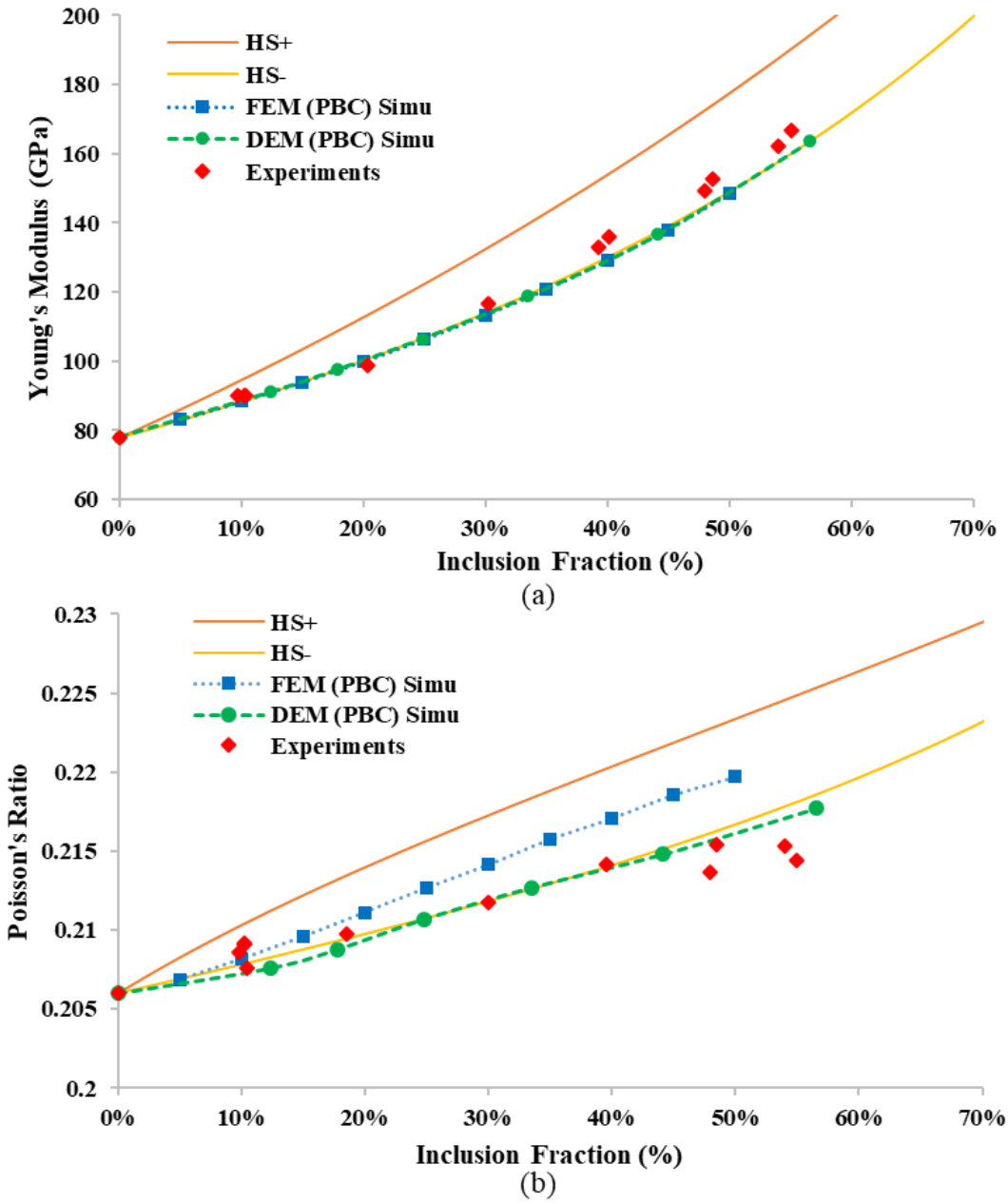

Fig. 9. DEM periodic homogenisation results compared to other predictive approaches and real experimental data for the bi-phase material, (a) apparent Young's modulus (E^{ap}) and (b) apparent Poisson's ratio (ν^{ap})

As can be seen in Fig. 9 (a), the DEM simulation using PBC and FEM periodic homogenisation are in perfect accordance with HS lower bound (HS-). Also, the experimental points are following the HS lower bound too, but with a slight tendency to the middle range of HS bounds for the higher inclusion fractions. Regarding Fig. 9 (b), although the HS bounds width was small (values between 0.2 and 0.23), the DEM model more accurately predicted the apparent Poisson's ratio of the bi-phase material, which is more coherent with the experimental results as well. The DEM model shows a smaller deviation compared to the FEM model, especially modelling the apparent Poisson's ratio. These results validate the potential of DEM for solving multiscale problems by using periodic homogenisation. The proposed method and the associated algorithm procedures constitute a promising route for a better understanding of the thermomechanical behaviour of heterogeneous materials.

Overall, the proposed DEM approach, combined with periodic homogenisation technique, leads to valid elastic properties determination for bi-phase and porous materials. These key results open very interesting new ways to use DEM to predict the thermomechanical behaviour of heterogeneous materials containing numerous microcracks that could propagate simultaneously. In fact, the fracturing process and microcracking simulations are among the key interests of using DEM in such a case compared to FEM. Therefore, the next section will be focused on the simulation of simultaneous microcracking in a continuum media that could be induced by thermal expansion mismatch between constituents.

European Commission | Horizon 2020 European Union funding for Research & Innovation

4 Modelling the Non-Linear Quasi-Brittle Behaviour of Heterogenous refractories by DEM

This study aims to use the Discrete Element Method (DEM) for simulating the fracture mechanisms in refractory ceramics that exhibit quasi-brittle behaviour and crack branching. Here again, the Flat-Joint DEM Contact Model (FJM), is used. In fact, fracture propagation requires a large number of discontinuities, and the Finite Element Method (FEM) is not easily capable of managing this kind of microstructural effects. Using DEM to model fracture mechanisms in a pseudo-continuum media, especially in the ceramics field, is a new and promising approach under active development.

Even if PFC with FJM is well-adapted to account for multiple crack propagation within a quasi-brittle material, unfortunately up to now, this model is not able to account for mechanical interactions and temperature variation simultaneously. This current limitation is a significant drawback (which is supposed to be resolved soon by ITASCA) to model refractory materials, which contain initial defects coming from CTE mismatch between constituents during the cooling stage after sintering. To overcome this current drawback, the present study investigated a randomisation of local fracture criteria within the virtual sample using a Weibull distribution (see section 4.1). The key idea is here to verify if the non-linear mechanical behaviour of a continuum media (see Fig. 10), can be reproduced by an initial well distributed damage (with a strengths dispersion following a Weibull distribution). This approach could enable the effect of pre-existing microcracks on the non-linear quasi-brittle behaviour of a sample under uniaxial tensile test to be studied. In addition, cyclic loadings were virtually performed (not presented here) to observe and verify the non-linear behaviour of the numerical sample, generally observed for quasi-brittle materials such as refractories. Finally, the wedge splitting test was considered as an application to verify the efficiency of this numerical technique by comparison with DIC outputs and calculation of the brittleness number of the samples. As a perspective, the proposed approach promotes a new numerical method that may be used to design and simulate an optimal microstructure in order to reduce brittleness in refractory ceramics.

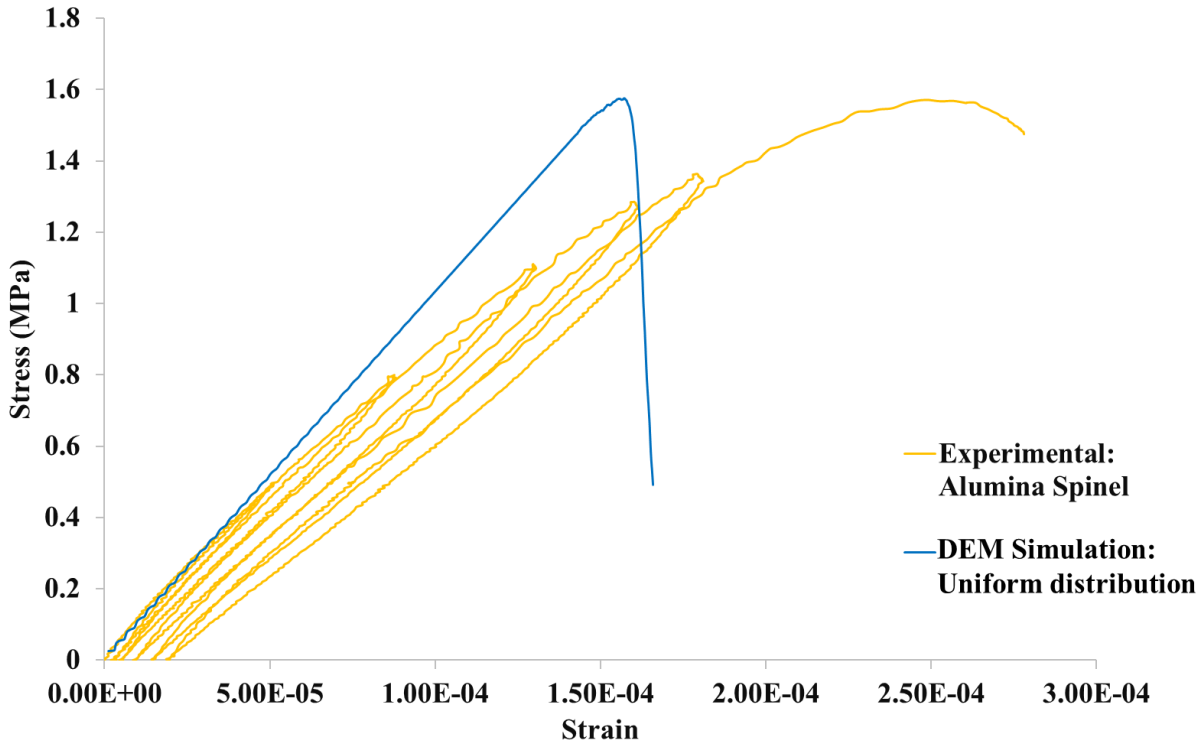

Fig. 10. Typical DEM simulation vs experimental results for a uniaxial tensile test.

4.1 Implementation of Weibull distribution to the mesoscale strength of bonds

Waloddi Weibull introduced this statistical distribution function in 1939 [12], and later, he proposed a better summarisation of his work in 1951 [13]. Afterwards, this distribution became widely used for different mechanical applications. By using Weibull distribution, the probability of failure for a solid material under a tensile load $P_f(\sigma)$ is given as [13]:

European Commission | Horizon 2020 European Union funding for Research & Innovation

$$P_f(\sigma) = 1 - e^{-\left(\frac{\sigma}{\sigma_0}\right)^m} \quad \text{Eq. 1}$$

where σ, m and σ_0 are the tensile stress (MPa), the Weibull modulus, and the scaling parameter, respectively.

The Weibull statistical distribution is commonly used as a macroscopic concept to describe the occurrence of random homogenised defects inside a 3D solid sample, which could cause a variation in the macroscopic tensile strength of the different specimens of a given material. In the field of ceramics, the Weibull modulus can exhibit a wide range, but is typically below 30.

In this study, this concept is used in the DEM simulations by using the local bond tensile strength (t^{loc}) of the Flat Joint contact model. It is proposed to reproduce the microscopic defects within the DEM numerical sample by a randomisation of the local bond tensile strength (t^{loc}) values. It means that the local bond tensile strength (t^{loc}) values follow a Weibull distribution law, defined by Eq. 1, where σ is considered as the local bond tensile strength (t^{loc}). In this way, the impact of this local randomisation will be investigated on the macroscopic non-linear behaviour of the refractory under tensile loadings, which in reality, originates from defects caused by thermal expansion mismatch between the refractory constituents.

The impact of applying randomisation on the local bond tensile strength (t^{loc}) is studied on pure magnesia as reference material. Pure magnesia exhibits a brittle behaviour with an apparent tensile strength of 6.5 MPa [14], which corresponds to the t^{loc} value of 6 MPa in the case of uniform distribution (where *m* = *infinite*). This value of 6 MPa is used as the scaling parameter (σ_0), in the Weibull equation (Eq. 1). It should be noted that, contrary to the normal distribution, the Weibull distribution is not a symmetrical statistical distribution in its domain. Hence, the scaling parameter (σ_0) of Weibull distribution is not the mean value of the domain. Afterwards, to study the impact of Weibull modulus *m* on the behaviour, three different values of *m* were tested: 3, 5 and *infinite*. The Weibull distribution and its relative parameters were introduced to the initial numerical sample using the NumPy[3] library in the Python environment. By keeping the scaling parameter constant (6 MPa), the t^{loc} distributions for the different considered Weibull modulus (*m* = 3, 5 and *infinite*) is shown in the upper part of Fig. 11. In addition, the 3D distribution of t^{loc} value within the numerical sample is shown in the lower part of Fig. 11.

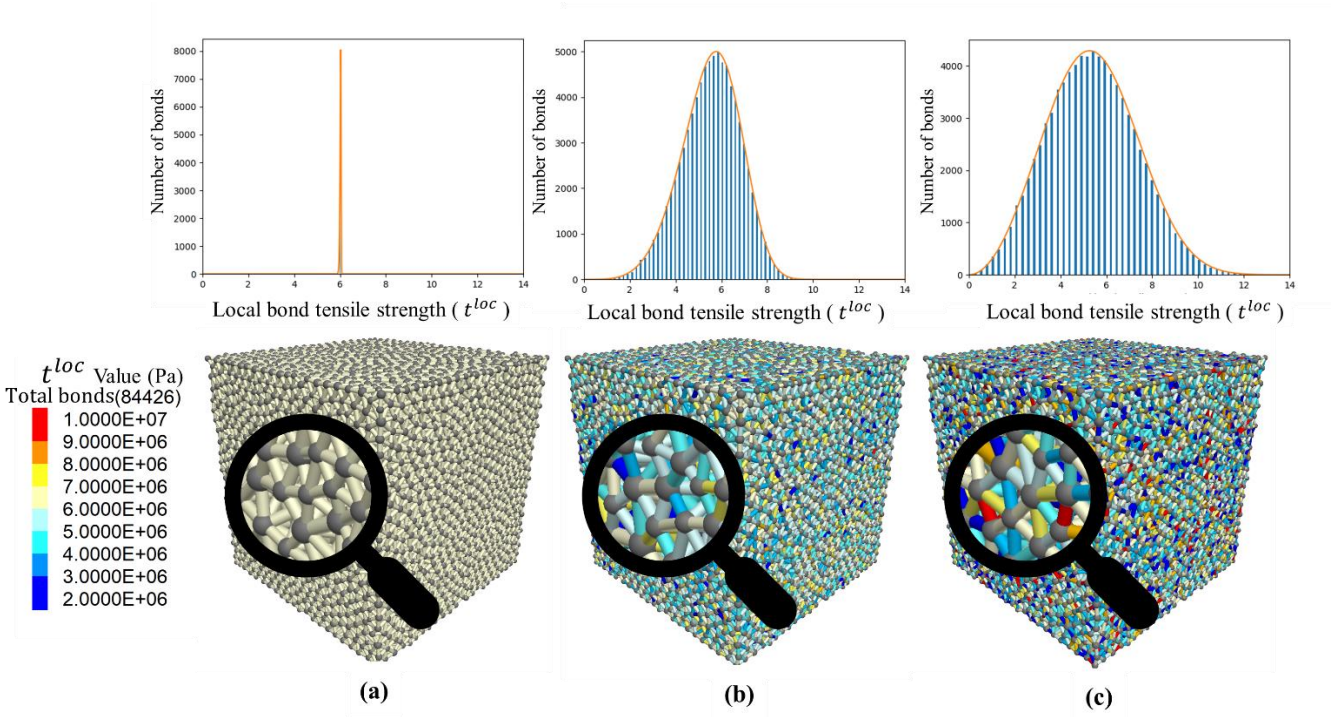

Fig. 11. The Weibull distribution curve and 3D distribution of t^{loc} value within the numerical specimens: (a) *m* = *infinite* (uniform distribution), (b) *m* = 5 and (c) *m* = 3.

In Fig. 11, the contact in the sample with uniform value of 6 MPa for the t^{loc} (*m* = *infinite*) is shown in cream white (a). While, the contacts in the sample with low Weibull modulus (*m* = *3*) are coloured in scale, based on their difference from 6 MPa (c). As

[3] https://numpy.org/

European Commission | Horizon 2020 European Union funding for Research & Innovation

all three samples are plotted based on the same colouring scale, the brighter the sample is, the higher is the Weibull modulus. The influence of Weibull modulus on the stress-strain curve of the uniaxial tensile test has been shown in Fig. 12.

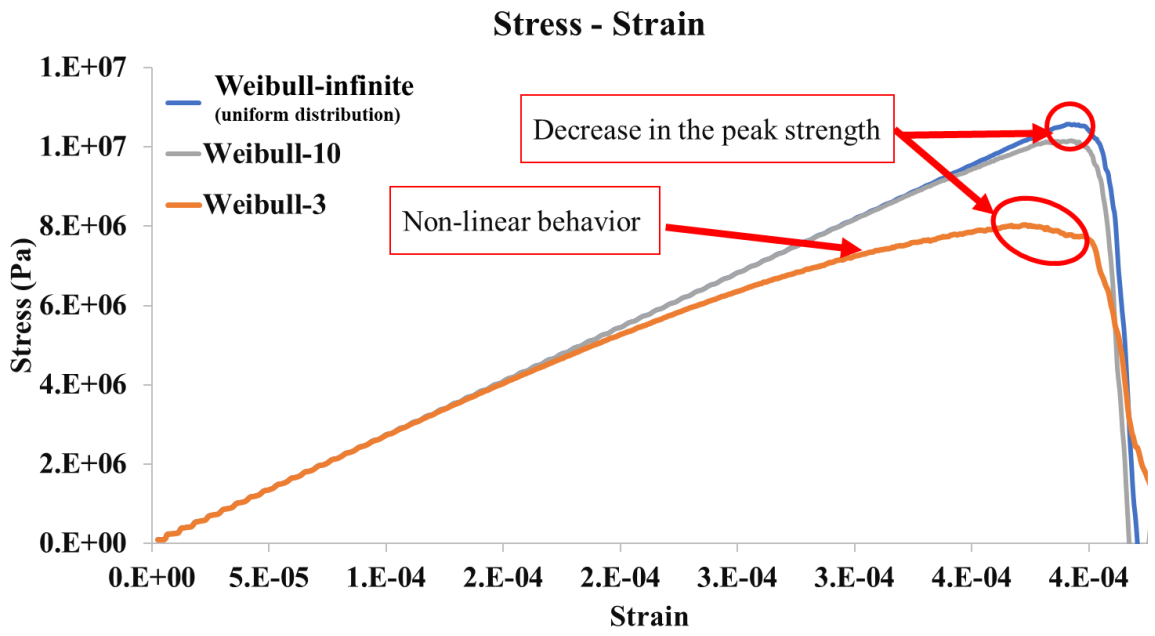

Fig. 12. The influence of Weibull modulus on the stress-strain curve of the uniaxial tensile test.

Fig. 12 shows that using Weibull distribution to randomise t^{loc} had a strong influence on the mechanical behaviour of the numerical samples. Low values of Weibull modulus (m), promoted non-linearity in the behaviour of the sample during tension. This process is quite similar to the phenomena that explain the quasi-brittle behaviour of certain refractory materials. However, as is shown in Fig. 12, in the same time, the Weibull modulus has a strong influence on the ultimate strength of the numerical sample. In order to achieve quantitative simulations of the non-linear behaviour of such real material, a robust calibration method is proposed in the next section.

4.2 Quantitative calibration process for non-linear behaviour of Alumina Spinel Refractory

Although in literature, the Weibull distribution has been used to model damaged materials [15] [16] [17], there is no definitive direct calibration algorithm. The proposed numerical technique has shown the ability to qualitatively introduce non-linear behaviour to the DEM numerical sample by using Weibull distribution over the t^{loc}. Now, to take the transitional step, from qualitative results to quantitative results, it is necessary to introduce a robust calibration process for reproducing the non-linear behaviour of refractory ceramics.

To highlight the quasi-brittle behaviour, the Alumina Spinel brick, which exhibits strong non-linearity, was chosen as a reference material to validate the proposed calibration process. As a preliminary step, the calibration algorithm for a perfect brittle material was used in order to achieve the initial apparent Young's modulus (E^{ap}), apparent Poisson's ratio (v^{ap}) and apparent uniaxial tensile strength (t^{ap}) of the material (as shown in Fig. 10). This preliminary calibration step has successfully achieved the right values of failure strength. At the foot of the curve, the simulated curve fits the experimental one, which means that the initial Young's modulus value was successfully calibrated. On the other hand, the simulation did not exhibit any quasi-brittle behaviour. Therefore, it is necessary to revise and introduce further calibration steps by using the Weibull distribution to model the non-linear behaviour quantitatively.

4.2.1 Quantifying non-linear behaviour

The first step to adjust and calibrate the observed non-linearity in the stress-strain curve of the model material is to assess and quantify it. In this regard, for a quasi-brittle material that promotes non-linear behaviour, the secant modulus (E^s) at the peak failure was considered to determine the evolution of the material's rigidity. By calculating the secant modulus (E^s) at the peak and having the initial elastic apparent Young's modulus (E^{ap}), which has been measured at the early stages of loading, quantifies the rate of Young's modulus decrease. This decrease comes from the non-linear behaviour of the materials induced by the increase of defects and microcracking process within the material during the progressive tensile loading. The initial apparent Young's modulus (E^{ap}) and peak secant modulus (E^s) has been shown and calculated in Fig. 13 for the Alumina Spinel model material.

European Commission | Horizon 2020 European Union funding for Research & Innovation

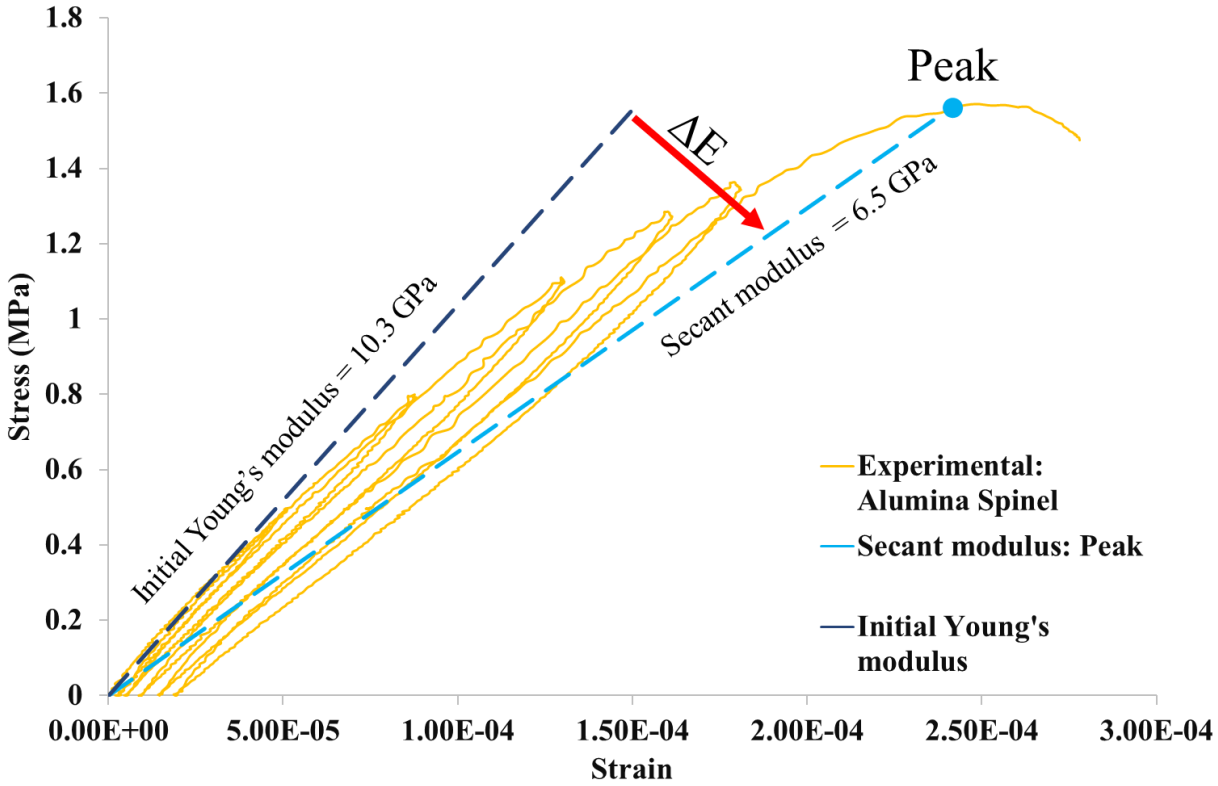

Fig. 13. Decrease of the rigidity of Alumina Spinel after six cycles of uniaxial tensile loadings.

As shown in Fig. 13, for the Alumina Spinel model material, the initial Young's modulus is 10.37 GPa. After being subjected to six cycles of uniaxial tensile loadings, the secant modulus of the peak has been reduced to 6.47GPa. This indicates the rigidity of the material after cyclic loadings has decreased to 62.4% of its initial value. The method used to quantitatively calibrate the input parameters to reproduce the experimental mechanical behaviour of such refractory is explained in the next sections.

4.2.2 *Calibrating the apparent linear behaviour*

Prior to calibrating the non-linear part of the stress-strain curve of Alumina Spinel (As shown in Fig. 13), the initial linear properties of the material should be calibrated. For this purpose, the behaviour of the material at the very beginning of the uniaxial tensile loading was considered. Then, by using the proposed calibration algorithm in Fig. 4 for FJM, the linear brittle parameters of the numerical model can be calibrated. The result of this calibration is shown in Fig. 10, and it should be highlighted that this result is without considering non-linear quasi-brittle behaviour.

4.2.3 *Calibrating the apparent non-linear behaviour*

After calibrating the initial linear properties, it was essential to calibrate the non-linear part of the stress-strain curve of the Alumina Spinel refractory. The process of quantifying the non-linear behaviour of such refractory under the uniaxial tensile loading was explained in section 4.2.1. To calibrate the non-linear behaviour, a Weibull distribution was used to vary the t^{loc} within the numerical sample. Briefly, introducing such statistical variation to the t^{loc} and decreasing *m* (while keeping the scaling parameter constant), had two impacts on the apparent mechanical behaviour of the numerical sample, it:

1. increased the non-linearity of the stress-strain curve, which is coming from the microcracking process and,
2. decreased the apparent tensile strength of the material due to the presence of an extensive microcrack network.

Regarding these points, to be able to use the Weibull distribution technique for simulating this quasi-brittle behaviour, the relationship between *m* and the non-linear behaviour of the material was studied. By investigating this relationship, the equivalent experimental non-linear behaviour was reproduced by the DEM numerical sample.

As the second step, despite the accordance of the non-linear behaviour, the apparent tensile strength of simulation was not equal to the experimental result. Therefore, the relationship of scaling parameter (σ_0) of Weibull distribution (which relates to the t^{loc}) with the apparent tensile strength had been studied. By investigating this relationship, it was possible to reproduce the same apparent tensile strength as the real Alumina Spinel refractory. The result of these calibrated parameters has been compared to the real experimental results for Alumina Spinel in the next section.

European Commission | Horizon 2020 European Union funding for Research & Innovation

4.2.4 Real case verification: simulation of Alumina-Spinel uniaxial tensile test

After going through the proposed calibration steps for non-linear behaviour, the simulation shows an excellent qualitative and quantitative accordance with the experimental results of Alumina Spinel brick, as shown in Fig. 14. The stress-strain curve of the simulation starts with the same initial Young's modulus. Afterwards, it promotes non-linear behaviour, following the pushovers of the cyclic loadings of the experimental curves. Then, it fails at the same tensile strength as the real material and, at the end, it predicts a reasonable post-peak failure behaviour of the material.

Overall, the proposed procedure for calibrating the DEM model to reproduce the non-linear behaviour of the quasi-brittle materials has been validated through comparison with real experimental results. The summary of the proposed calibration process for non-linear behaviour can be proposed as a numerical algorithm. Such a numerical algorithm could potentially be applied to other DEM bond models and other bond strength distribution laws. The proposed numerical approach can also be used to tune the fracture branching process and, consequently, the fracture energy of the model materials. Therefore, in the next section, this approach is also applied to the Wedge Splitting Test (for which the majority of the microcracks that occur are in mode I) to verify this point.

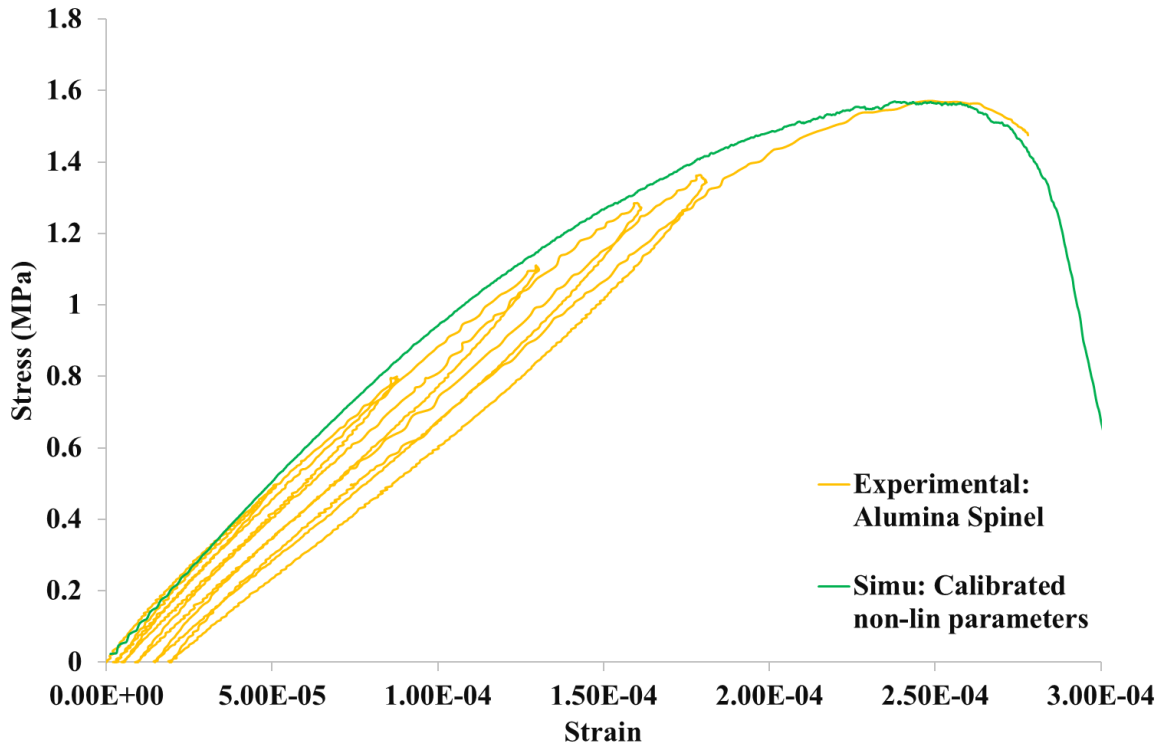

Fig. 14. DEM simulation (using the proposed numerical approach for modelling non-linear mechanical behaviour) vs real Alumina Spinel experimental non-linear behaviour under uniaxial tensile loading.

5 Modelling the quasi-brittle behaviour during Wedge Splitting Test

In the refractory field, the mechanical test which is used for fracture mechanics studies is the Wedge Splitting Test (WST). The principle of this test is to open a notch by inserting a wedge, in a displacement driven experiment, to produce a stable fracture propagation. This test gives more information about fracture energy and brittleness number of the material [18]. Specific fracture energy is the amount of energy necessary to create a one-unit area of a crack. Recent developments, in combination with Digital Image Correlation (DIC), enable the monitoring of crack branching during the WST [20]. In fact, the pre-existing microcracks and crack branching play a key role in the enhancement of the fracture energy of the material. To summarise, WST results could be used as an index for characterising the fracture behaviour of quasi-brittle refractories.

5.1 Mimicking microcrack branching and qualitative comparison to the experimental DIC outputs

Based on a previous study of the fracture behaviour of pure MgO and Magnesia Hercynite (15% Hercynite - MH15) by Khlifi [21], the Two Parts-DIC (2P-DIC) technique was used to detect and visualise the crack propagations during WST. As stated, pure MgO and MH15 were interesting materials for this analysis as they could highlight a wide range of fracture behaviours, from a

European Commission | Horizon 2020 European Union funding for Research & Innovation

brittle material to a quasi-brittle. In the mentioned study, the displacement fields within the WST sample were measured throughout the test in order to visualise crack propagation during loading.

In the present study, numerical modelling has been managed in order to mimic this WST experiment. Two virtual samples were thus constructed: one with a uniform value of 6 MPa for the local tensile strength to exhibit the Pure MgO brittle behaviour, and the other one, using a Weibull distribution (m = 3) of the local tensile strength, to exhibit the MH15 quasi-brittle behaviour. Fig. 15 shows these two samples at the end of the simulations.

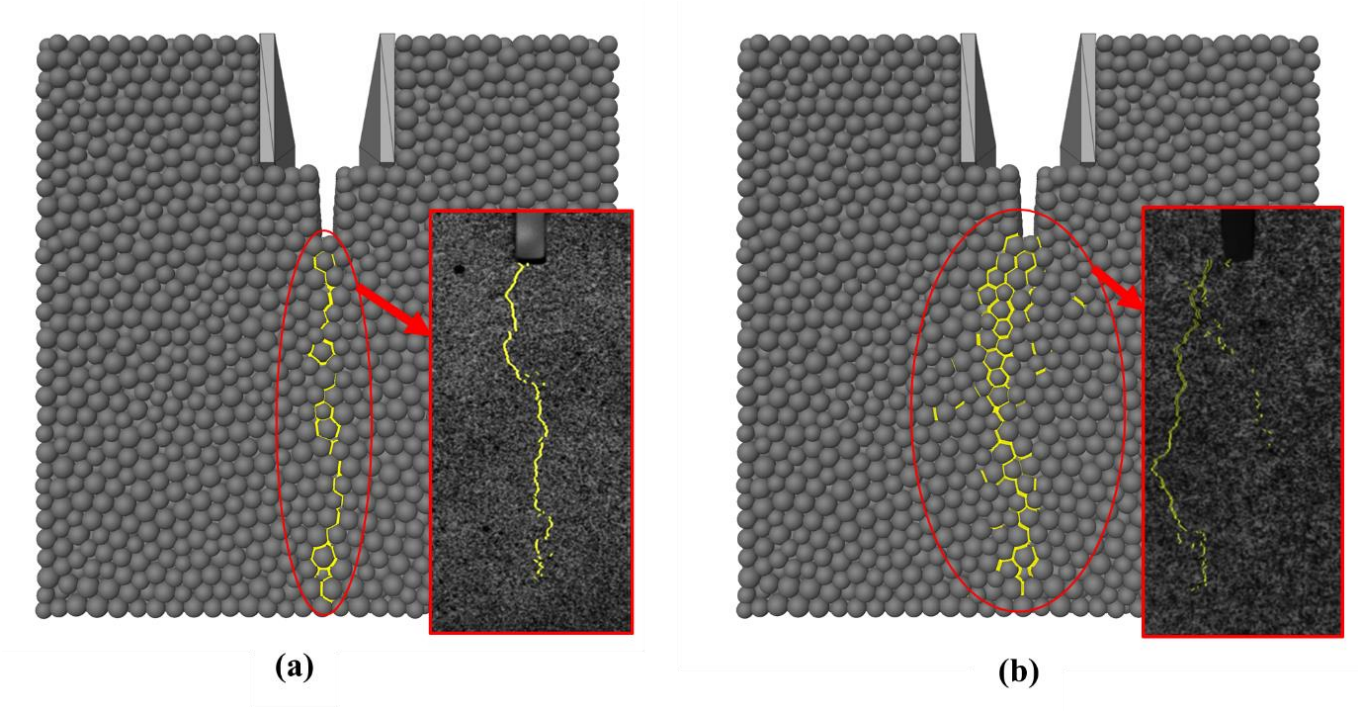

Fig. 15. Comparison of the crack paths from DEM simulation vs DIC outputs (in the red frame): (a) case of pure MgO with a rather straight crack path, (b) case of MH15 with a deviated crack path. DIC results from Khlifi et al. [22]

At first glance, it shows that in the simulation of the pure MgO, the sample was broken with a rather straight fracture path, without any crack branching, which is underlining a highly brittle material. On the other hand, in the simulation of the MH15, the sample exhibits a deviated crack path and crack branching, which is due to the quasi-brittle behaviour of the material. Overall, these results are showing acceptable qualitative fracture behaviour in comparison to the real materials, which confirms the applicability of the proposed DEM numerical approach in WST. In fact, by using this approach, the numerical models could dissipate more energy through the initiation of microcracks and crack branching, which results in a higher fracture energy for the quasi-brittle samples.

5.2 Impact on fracture energy and brittleness number

The force-displacement curves of WSTs of the previous section have been plotted. After treatment and analysis of the obtained results and curves for the WST simulation, a quantitative verification was considered. For this purpose, the brittleness number was used as an indicator for the brittleness of refractories [23]. The force-displacement diagrams were used to calculate the brittleness number in this numerical study (Fig. 16).

European Commission | Horizon 2020 European Union funding for Research & Innovation

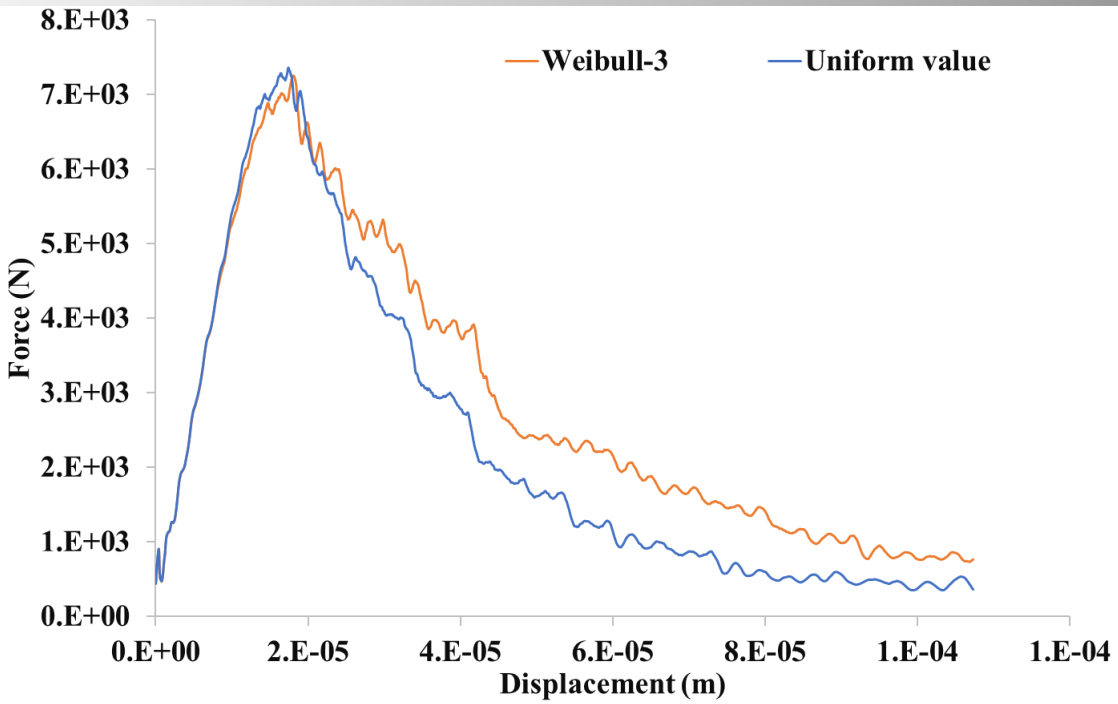

Fig. 16. Comparison of the force-displacement diagrams for wedge splitting test for two samples.

The calculated brittleness number for the MH15 numerical sample (m = 3) is 0.38, whereas, for the pure MgO numerical sample (with a uniform value for the local tensile strength), the brittleness number is 0.55. These results confirm that using Weibull distributions for local tensile strength influences the brittleness of the sample. Moreover, by using Weibull distributions, the post-peak area in the force-displacement is enlarged, which is correlated to a higher fracture energy.

Overall, random local strength distributions in DEM models, such as Weibull distributions, which were used in the present study, could be used to calibrate the amount of fracture energy and its related brittleness number. This procedure could help to design and simulate optimal microstructures, accounting for pre-existing microcracks. At the macro-scale, this approach could reproduce the quasi-brittle behaviour and brittleness reduction in refractory ceramics.

6 Conclusion

To conclude, new DEM numerical approaches have been proposed and developed to investigate the influence of material microstructure on macroscopic thermomechanical behaviour. Firstly, a DEM periodic homogenisation approach was proposed and validated by comparing to model materials, analytical and FEM models. This approach allows an accurate micro to macro multiscale transition of elastic properties. Secondly, a DEM model proposed to use a statistical approach to mimic microcracks, which could potentially come from thermal expansion mismatches. This later technique was also confronted and validated by Alumina Spinel mechanical test data. Finally, to check the applicability of the proposed DEM models, WST simulations were qualitatively compared to DIC experimental outputs.

These proposed numerical techniques could be used to promote a new multiscale numerical approach, helping to design and simulate optimal microstructures, accounting for pre-existing microcracks which promote quasi-brittle behaviour in refractory materials.

7 References

[1] D. O. Potyondy, 'A flat-jointed bonded-particle material for hard rock', presented at the 46th U.S. Rock Mechanics/Geomechanics Symposium, Jan. 2012, Accessed: Jul. 09, 2020. [Online]. Available: https://www.onepetro.org/conference-paper/ARMA-2012-501.

[2] Itasca Consulting Group Inc., 'PFC2D/3D Version 6.0 Documentation'. Itasca Consulting Group Inc., 2020.

[3] Vallejos Javier Andres, Salinas José Matias, Delonca Adeline, and Mas Ivars Diego, 'Calibration and Verification of Two Bonded-Particle Models for Simulation of Intact Rock Behavior', *Int. J. Geomech.*, vol. 17, no. 4, p. 06016030, Apr. 2017, doi: 10.1061/(ASCE)GM.1943-5622.0000773.

European Commission | Horizon 2020 European Union funding for Research & Innovation

[4] C. Zhou, C. Xu, M. Karakus, and J. Shen, 'A systematic approach to the calibration of micro-parameters for the flat-jointed bonded particle model', *Geomech. Eng.*, vol. 16, no. 5, pp. 471–482, 2018, doi: 10.12989/gae.2018.16.5.471.
[5] N. Tessier-Doyen, J. C. Glandus, and M. Huger, 'Experimental and numerical study of elastic behavior of heterogeneous model materials with spherical inclusions', *J. Mater. Sci.*, vol. 42, no. 14, pp. 5826–5834, Jul. 2007, doi: 10.1007/s10853-006-1386-8.
[6] N. Tessier-Doyen, 'Etude expérimentale et numérique du comportement thermomécanique de matériaux réfractaires modèles', thesis, University of Limoges, Limoges, France, 2003.
[7] P. A. Cundall, 'Computer Simulations of Dense Sphere Assemblies', in *Studies in Applied Mechanics*, vol. 20, M. Satake and J. T. Jenkins, Eds. Elsevier, 1988, pp. 113–123.
[8] R. Grasset-Bourdel *et al.*, 'Optimisation of 3D RVE for anisotropy index reduction in modelling thermoelastic properties of two-phase composites using a periodic homogenisation method', *Comput. Mater. Sci.*, vol. 50, no. 11, pp. 3136–3144, Oct. 2011, doi: 10.1016/j.commatsci.2011.05.042.
[9] S. Brisard, L. Dormieux, and D. Kondo, 'Hashin–Shtrikman bounds on the bulk modulus of a nanocomposite with spherical inclusions and interface effects', *Comput. Mater. Sci.*, vol. 48, no. 3, pp. 589–596, May 2010, doi: 10.1016/j.commatsci.2010.02.027.
[10] R. S. Lakes, *Viscoelastic Solids*. CRC Press, 1998.
[11] C. Tucker and E. Liang, 'Stiffness Predictions for Unidirectional Short-Fiber Composites: Review and Evaluation', *Compos Sci Technol*, pp. 59–655, 1999.
[12] W. Weibull, *The phenomenon of rupture in solids,*. Generalstabens litografiska anstalts foÌˆrlag, 1939.
[13] W. Weibull, 'A Statistical Distribution Function of Wide Applicability', *Journal of Applied Mechanics*, vol. 18, pp. 293–297, 1951.
[14] R. Grasset-Bourdel, 'Structure/property relations of magnesia-spinel refractories : experimental determination and simulation', These de doctorat, University of Limoges, Limoges, France, 2011.
[15] C. Zhou, M. Karakus, C. Xu, and J. Shen, 'A new damage model accounting the effect of joint orientation for the jointed rock mass', *Arab. J. Geosci.*, vol. 13, no. 7, p. 295, Mar. 2020, doi: 10.1007/s12517-020-5274-3.
[16] H. Liu and X. Yuan, 'A damage constitutive model for rock mass with persistent joints considering joint shear strength', *Can. Geotech. J.*, vol. 52, no. 8, pp. 1136–1143, Jan. 2015, doi: 10.1139/cgj-2014-0252.
[17] X. Li, W.-G. Cao, and Y.-H. Su, 'A statistical damage constitutive model for softening behavior of rocks', *Eng. Geol.*, vol. 143–144, pp. 1–17, Aug. 2012, doi: 10.1016/j.enggeo.2012.05.005.
[18] E. K. Tschegg, 'Equipment and appropriate specimen shape for tests to measure fracture values', AT-390328, 1986.
[19] K. Duan, X. Hu, and F. H. Wittmann, 'Size effect on specific fracture energy of concrete', *Eng. Fract. Mech.*, vol. 74, no. 1, pp. 87–96, Jan. 2007, doi: 10.1016/j.engfracmech.2006.01.031.
[20] J.-C. Dupré, P. Doumalin, Y. Belrhiti, I. Khlifi, O. Pop, and M. Huger, 'Detection of cracks in refractory materials by an enhanced digital image correlation technique', *J. Mater. Sci.*, vol. 53, no. 2, pp. 977–993, Jan. 2018, doi: 10.1007/s10853-017-1550-3.
[21] I. Khlifi, 'Optimisation of optical methods for strain field measurements dedicated to the characterisation of the fracture behaviour of refractories : Application to magnesia based materials', These de doctorat, University of Limoges, Limoges, France, 2019.
[22] I. Khlifi, O. Pop, J.-C. Dupré, P. Doumalin, and M. Huger, 'Investigation of microstructure-property relantionships of magnesia-hercynite refractory composites by a refined digital image correlation technique', *J. Eur. Ceram. Soc.*, vol. 39, no. 13, pp. 3893–3902, Oct. 2019, doi: 10.1016/j.jeurceramsoc.2019.05.010.
[23] H. Harmuth and E. K. Tschegg, 'A Fracture Mechanics Approach for the Development of Refractory Materials with Reduced Brittleness', *Fatigue Fract. Eng. Mater. Struct.*, vol. 20, no. 11, pp. 1585–1603, 1997, doi: 10.1111/j.1460-2695.1997.tb01513.x.

European Commission | Horizon 2020 European Union funding for Research & Innovation